Ab Initio Study of the Electron Transfer in an Ionized Stacked Complex of Guanines

Emilie Cauët* and Jacques Liévin

Service de Chimie Quantique et Photophysique, Université Libre de Bruxelles, CP 160/09, 50 Avenue F.D. Roosevelt, B-1050 Bruxelles, Belgium

Received: March 18, 2009; Revised Manuscript Received: July 6, 2009

The charge transfer process in an ionized stacking of two consecutive guanines $(G_{5'}G_{3'})^+$ has been studied by means of state-averaged CASSCF/MRCI and RASSCF/RASPT2 calculations. The ground and two first excited states of the radical cation have been characterized, and the topology of the corresponding potential energy surfaces (PESs) has been studied as a function of all intermolecular geometrical parameters. The results demonstrate that the charge transfer process in $(G_{5'}G_{3'})^+$ is governed by the avoiding crossing between the ground and first excited states of the complex. Relative translation motions of both guanines in their molecular planes are shown to lead to the charge migration between $G_{5'}$ and $G_{3'}$. Five stationary points (three minima and two saddle points) have been characterized along the reaction path describing the passage of the positive charge from $G_{5'}$ to $G_{3'}$. The global minimum on the PES is found to correspond to the charge configuration $G_{5'}{}^+G_{3'}$. The existence of an intermediate minimum along the reaction path has been established, characterizing a structure where the positive charge is equally distributed between the two guanines. The calculated energy profile allowed us to determine the height of the potential energy barrier (7.33 kcal/mol) and to evaluate the electronic coupling at a geometry close to the avoiding crossing (3.6 kcal/mol). Test calculations showed that the topology of the ground state PES of the complex GG^+ is qualitatively conserved upon optimization of the intramolecular geometrical parameters of the stationary points.

1. Introduction

In recent years, electron transfer in DNA has attracted considerable attention and has been the subject of intense research because of its importance in mechanisms of DNA damage caused by oxidizing agents and photoirradiation.[1−4] In addition, electron transfer reactions through DNA have important applications to the construction of DNA-based sensors and nanoscale devices.[5−7] It is now well recognized that the charge migration is mediated by the $\pi-\pi$ interactions between the stacked DNA bases.[8,9] Two different mechanisms for the hole transfer in DNA have been proposed, namely, the superexchange and the hopping mechanisms.[10−15] The single-step superexchange mechanism[10−12] is relevant for the short-range charge transfer (10−15 Å), whereas the multistep hole hopping mechanism[12−15] may be treated as a series of superexchange steps between DNA bases separated by much larger distances (up to hundreds of angstroms). The fact that guanine (G) is the most easily oxidized nucleobase suggests that the radical cation G^+ is a key intermediate in the hole transfer process mediated by DNA. Created initially adjacent to an oxidant, the charge hops through the DNA base stack using guanines as stepping stones.[12,14] A detailed investigation of the elementary step in which a positive charge migrates from one guanine to another is thus fundamental for understanding how the charge transfer occurs through long DNA base sequences.

For many years, there have been abundant experimental[9,12,14,16−22] and theoretical investigations[23−31] devoted to the refinement of the charge transfer models between G sites. Key parameters of the hole transfer models are the energies of the nucleobase cation radicals and the electronic couplings between the stacked nucleobases. Several theoretical studies have been performed to calculate the ionization energies of the DNA bases embedded in the Watson−Crick base pairs [32−37] in stacked clusters[38−45] and to investigate the charge delocalization in DNA base clusters.[46−51] Different models based on quantum chemical calculations have been proposed and reported in the literature to estimate the hole transfer electronic couplings in DNA stacks.[28−30] These models usually assume the validity of the two-state approximation, in which the space of the two states of interest (i.e., the two states in which the hole is localized alternatively in one of two DNA bases) is well separated energetically from the other states of the system.[52] Only a few studies that deal with a multistate approach have been published so far.[53−55] In most cases, Hartree−Fock wave functions have been used[27−29,51,56−60] and Koopmans' theorem approximation has been applied.[27−29,51,56−58] Within this scheme, the properties of the states of the radical cation are evaluated using the difference of the one-electron energies of the highest occupied molecular orbitals calculated for the corresponding neutral system. In the same way, the couplings have been calculated using density functional theory.[47] Beyond the one-electron approximation, some studies have used multiconfigurational wave functions.[61−63] Blancafort et al.[61] employed the CASSCF and CASPT2 methods to calculate the ground and excited states of radical cations consisting of two and three nucleobases. Using the results as reference data, these authors also tested the application of several semiempirical methods in the calculation of electronic couplings in DNA π-stacks, showing that only the method INDO/S gives reliable results.[31,64] Recently, the MS-PT2 and TD-DFT methods have been tested for calculating electronic states of corresponding radical anions.[62,63]

In all of the above-mentioned theoretical studies, arbitrary molecular geometries of DNA base stacks, which are supposed to be favorable to charge transfer, were used to calculate the couplings. Some of them have analyzed the changes of the electronic couplings associated with the DNA structural fluctua-

* Corresponding author. E-mail: ecauet@ulb.ac.be.

10.1021/jp902426p CCC: $40.75
Published on Web 08/14/2009

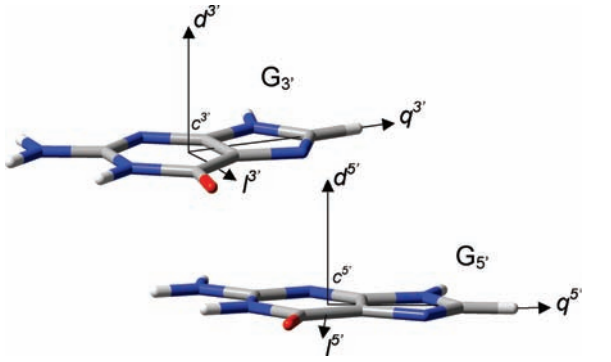

Figure 1. Definition of local reference coordinate systems ($l^{5'}$, $q^{5'}$, $d^{5'}$) and ($l^{3'}$, $q^{3'}$, $d^{3'}$) for the guanines located in the 5′ ($G_{5'}$) and 3′ ($G_{3'}$) directions, respectively. The geometry is taken from the X-ray structure of TC3 transposase (protein code 1TC3), and the interacting residues are Gua-A7 and Gua-A8. Atoms O, N, C, and H are colored in red, blue, gray, and white, respectively.

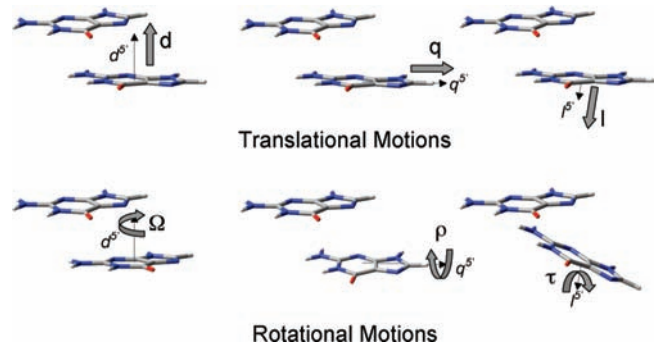

Figure 2. Definition of the intermolecular translations and rotations involving two consecutive DNA bases.

tions by selecting a series of static geometries from the available crystallographic data for DNA sequences.[59,65] Several authors also performed classical MD simulations to quantify the fluctuations of the charge transfer parameters with the DNA dynamics.[5,31,57,60,66−71] In most of these studies, the DNA structure fluctuations were assumed to occur only as changes in vertical separation and twisting motion of the base pairs of the DNA helix. The authors show that the charge transfer parameters exhibit large oscillations when computed for snapshots along classical MD trajectories. Whereas these studies highlight a strong dependence of the electronic coupling on the relative geometry of the nucleobases, the geometries of DNA base complexes that are expected to facilitate charge transfer have not completely been characterized. Therefore, the real role of the base motion on the mechanism of charge transfer is still not well understood, and the structural and energetic details of the potential energy surfaces (PESs) of the electronic states governing the charge transfer between two guanines still remain completely unknown. This issue is addressed in this article by considering the single-step charge transfer in an ionized stacking of two consecutive guanines $(GG)^+$. The topology of the adiabatic PES of the system $(GG)^+$ has been investigated as a function of a restricted set of geometrical parameters. High-level multiconfigurational calculations have been performed, providing an accurate representation of the wave functions along the reaction coordinate governing the charge migration. For the first time, the corresponding energy profile has been predicted and the conformational changes accompanying the charge transfer process have been identified.

This article is organized as follows. The geometrical model used in this work is defined in Section 2. The method of calculations and the computational strategy are developed in Section 3. Results and Discussion are presented in Section 4, before concluding in Section 5.

2. Geometrical Model

In this work, our model consists of an ionized stacking of two consecutive guanines $(GG)^+$, both guanines being in the same strand. We started from the X-ray geometry of TC3 transposase (protein code 1TC3, residues Gua-A7 and Gua-A8) used in our previous investigations on stair-motifs at the protein−DNA interfaces.[72,73] This structure is represented in Figure 1, where the guanines located in the 5′ and 3′ directions of the strand are labeled $G_{5'}$ and $G_{3'}$, respectively. The intramolecular geometrical parameters relative to each base were optimized at the HF/6-31G(d,p)[74,75] level of theory and kept fixed during all our calculations. Neglecting the coupling between the inter- and intramolecular geometrical parameters is justified by the fact that the process of interest is governed by the interactions between the delocalized π structures of the monomers and that this delocalization is assumed to be insensitive to intramolecular geometry changes. The "frozen monomers" approximation has been widely used in the literature for investigating the stability and reactivity of stacked π systems[73,76−80] and will be further discussed in Section 4.4. The intermolecular geometrical parameters have been defined with respect to local rectilinear reference coordinate systems ($l^{5'}$, $q^{5'}$, $d^{5'}$) and ($l^{3'}$, $q^{3'}$, $d^{3'}$) defined for the guanines $G_{5'}$ and $G_{3'}$, respectively. (See Figure 1.) The origins $c^{5'}$ and $c^{3'}$ of both systems are chosen to be the center of mass of each nucleobase. The d axes are perpendicular to the molecular planes and point in the 5′−3′ direction. The q axes are oriented along the CH bonds of the five-cycles of the bases, and the l axes point toward the CO bonds. The 1TC3 structure corresponds to a configuration in which the coordinates of $c^{3'}$ are (1.1, −2.9, 3.3) (in angstroms) in the ($l^{5'}$, $q^{5'}$, $d^{5'}$) coordinate system, and the $l^{3'}$, $q^{3'}$, and $d^{3'}$ axes are rotated by $\alpha = 27.75°$, $\beta = 27.33°$, and $\gamma = 6.26°$ with respect to $l^{5'}$, $q^{5'}$, and $d^{5'}$, respectively. Note that γ gives a measure of the nonparallelism between both guanine molecular planes, whereas α and β account for the DNA helicoidal step orientation.

Two notations are introduced corresponding to two distinct positions of the positive charge that may occur in the system $(G_{5'}G_{3'})^+$. In one position, denoted $G_{5'}{}^+G_{3'}$, the positive charge is on the guanine $G_{5'}$. In the second position, $G_{5'}G_{3'}{}^+$, the positive charge is on the guanine $G_{3'}$. In the present study, we explored the PES of the radical cation $(G_{5'}G_{3'})^+$ to find the local minima corresponding to the two repartitions of the charge: $G_{5'}{}^+G_{3'}$ and $G_{5'}G_{3'}{}^+$. Using the structure TC3 as reference geometry, we have investigated the reaction path connecting the minima and the height of the potential energy barrier that separates them by moving $G_{5'}$ with respect to $G_{3'}$, the latter nucleobase being kept fixed. Six intermolecular geometrical parameters are used for that purpose. (See Figure 2.) The parameters d, q, and l correspond to three translation motions applied to the center of mass of $G_{5'}$ in the directions of axes $d^{5'}$, $q^{5'}$, and $l^{5'}$, whereas the parameters Ω, ρ, and τ define the rotations of the $G_{5'}$ molecular plane around $d^{5'}$, $q^{5'}$, and $l^{5'}$ axes, respectively. Note that we consider that the ($l^{5'}$, $q^{5'}$, $d^{5'}$) system follows the translation motions of $G_{5'}$ without any reorientation. The parameters described above are well adapted to a single-strand stack. They could be related to the so-called local base-pair step parameters (Rise, Side, Shift, Twist, Roll, and Tilt)[81] by extending the model system to include the base pairs, guanine−cytosine, thus taking the cDNA strand into account.

3. Methods of Calculation

To survey the PES of the radical cation $(GG)^+$, multiconfiguration ab initio calculations have been performed using the 6-31G(d(0.2)) basis set[73] corresponding to the standard 6-31G basis set augmented by diffuse polarization functions ($\alpha_d = 0.2$) on the heavy atoms: oxygen, carbon, and nitrogen. We demonstrated in our previous work that this medium basis set is able to describe the stacking stability[73] and the electronic changes accompanying the ionization[44] as well as larger polarized and augmented basis sets of the literature but at lower computer costs. Complete[82−84] and restricted[85] active space self-consistent field (CASSCF and RASSCF) calculations have been performed in which the molecular orbitals playing an active role in the charge transfer process between the two guanines were optimized. A state-averaging procedure[82] has been used to optimize a common molecular orbital basis set describing the low-lying electronic states of the dimer $(GG)^+$. The choice of the states involved in the state averaging optimization was found to be particularly important and required careful investigation to represent properly the two states corresponding to the two repartitions of the charge $G_{5'}{}^+G_{3'}$ and $G_{5'}G_{3'}{}^+$ and all interacting states. Main configuration state functions (CSFs) defining these states have been accounted for in a restricted active orbital space correlating a minimal number of electrons. To introduce the remaining dynamical correlation, the CASSCF and RASSCF calculations have been followed by internally contracted multireference configuration interaction[86,87] (MRCI) and second-order perturbation theory[88−90] (RASPT2) calculations, respectively. All calculations were performed with the MOLPRO[91] program package running on the Compaq alpha servers of the ULB/VUB computer center. The Mulliken approach[92] has been employed for localizing the positive charge in the stacked cluster.

To elucidate the relative stability of the configurations corresponding to the stationary points on the PES of the radical cation $(GG)^+$, we calculated the interaction energies of the optimized geometrical structures at the MP2[93,94] level with the 6-31G(d(0.2)) basis set. The standard counterpoise method[95] was applied to correct the interaction energies for the basis set superposition error. These calculations were performed with the Gaussian03[96] program suite.

3.1. CASSCF/MRCI Calculations. An initial single excitation configuration interaction (CIS) test calculation carried out for the X-ray structure 1TC3 of the stacked dimer $(GG)^+$ suggests that the charge transfer process from a guanine to the other implies the progressive passage from the ground configuration to the first excited configuration. This prediction is in agreement with a large number of MRCI test calculations performed with different sets of configurations. The analysis of the MRCI wave functions of the low-lying states of the radical cation $(GG)^+$ shows that configuration mixing occurs within the ground, first, and second excited states of the dimer. The three lowest states are characterized by a dominant configuration corresponding to the singly occupied HOMO, $HOMO^{-1}$, and $HOMO^{-2}$ for the ground, first, and second excited states, respectively. These three molecular orbitals constitute the minimal active space for describing the electron transfer.

The size of the active orbital space will be defined by the standard notation $[n,m]\_x$ CASSCF indicating that n electrons are distributed in all possible ways among m molecular orbitals, with x being the number of states involved in the state averaging procedure. The minimal active orbital space *[5,3]_3* has been used in preliminary CASSCF calculations, presented in Section 4.1, where only one of the six intermolecular parameters of the cluster was changed. This space is defined by the three highest occupied molecular orbitals (HOMO, $HOMO^{-1}$, and $HOMO^{-2}$), in which five electrons are distributed to form the CASSCF wave functions. These wave functions provided the smaller multiconfigurational description of the three lowest states of the system. A significant amount of computer time is required for variationally optimizing the 75 closed shell orbitals in addition to the 3 active orbitals. For this reason, we decided to freeze the 36 lowest occupied molecular orbitals arising from the 1s and 2s orbitals of oxygen, carbon, and nitrogen, which were optimized at the SCF level. This results in a reduction of the computer time by a factor of three without significant loss of accuracy.

The state-averaged CASSCF calculations with the minimal active orbital space *[5,3]_3* were performed as a preliminary orbital optimization step to prepare for MRCI calculations. The multireference wave function used in the MRCI calculations exactly corresponds to the CASSCF wave function. All single and double excitations from the active orbitals to the external orbital space were included in the MRCI expansion, whose size reached 10^5 contracted CSFs. This level of calculation, noted CASSCF/MRCI(5) below in this work, takes into account both dynamical and nondynamical correlation effects of the five active electrons providing a correct representation of the electronic states of the radical cation $(GG)^+$. Small changes in configuration weights are observed for the CASSCF and CASSCF/MRCI wave functions. The detected mixings suggests that a weak interaction occurs between the main and doubly excited configurations, promoting electrons to the external orbital space. The energy difference between the ground and first excited states is 6.35 and 4.72 kcal/mol for the CASSCF and CASSCF/MRCI calculations, respectively. The Mulliken atomic populations calculated for these states show that the repartitions of the positive charge in the stacked dimer $(GG)^+$ are inverted for the MRCI results.

To validate the CASSCF/MRCI(5) level of theory, we performed CASSCF calculations with an active space extended to 11 electrons in 10 orbitals. The calculated first excitation energy reaches 4.40 kcal/mol, which confirms the CASSCF/MRCI value calculated with only three active molecular orbitals. One sees that the interaction between the three first electronic states and the highest excited states is properly described in the CASSCF/MRCI(5) calculation, whereas the CPU time is decreased by a factor of 2.5 relative to the CASSCF calculation with 11 active electrons.

3.2. RASSCF/RASPT2 Calculations. The multireference second-order perturbation theory (CASPT2 or RASPT2) has been shown to be adequate for correlating a substantial number of electrons. However the results of PT2 calculations are more sensitive to the choice of the MCSCF reference wave function, and convergence problems can occur if the active orbital space is not adequately chosen. The analysis of the *[5,3]_3* CASSCF/MRCI(5) wave functions has shown that couplings exist between the reference configurations and the excited configurations obtained by double electron promotions to the external orbital space. Therefore, to apply the PT2 theory, we enlarged the minimal active orbital space by including orbitals that are unoccupied in the HF wave function. To limit the increase of the CPU time, we have used the RASSCF method. The notation $\{R1[e,m_1]; R2[n,m_2]; R3[f,m_3]\}\_x$ RASSCF has been adopted for defining the splitting of the active orbital space into three standard subsets: RAS1, RAS2, and RAS3. This notation indicates, for each subset Ri, the number m_i of included molecular orbitals. The maximal number of excitations that can

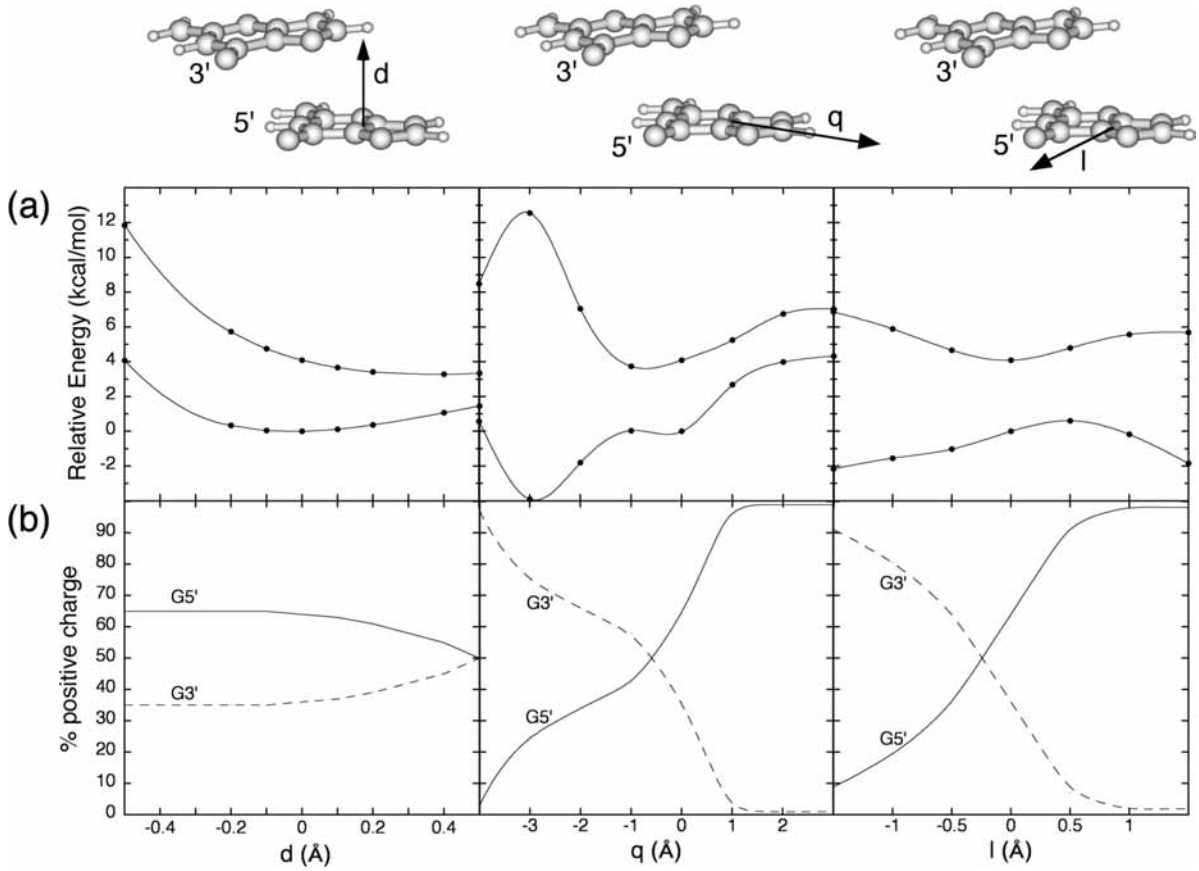

Figure 3. (a) Energies of the ground state and of the first excited state computed at the CASSCF/MRCI(5)/6-31G(d(0.2)) level for the stacked $(G_{5'}G_{3'})^+$ system as a function of the parameters *d*, *q*, and *l*. (b) Percentages of the positive charge on the guanine $G_{5'}$ (solid line) and on the guanine $G_{3'}$ (dotted line) calculated for the ground state as a function of the parameters *d*, *q*, and *l*.

be done from RAS1 is given by *e*, whereas *f* is the maximal number of excitations that can be done to RAS3. The number of electrons distributed in RAS2 is defined by *n*, whereas *x* is the number of states involved in the state averaging procedure.

In this work, no RAS1 space has been defined, and only double excitations have been allowed from RAS2, the minimal reference space [*5*,*3*], to RAS3. All RASSCF calculations have been done using the optimized [*5*,*3*]_*3* CASSCF orbitals as the initial one-electron basis set, and the same core of doubly occupied orbitals has been conserved. Test calculations have been performed to determine the number of molecular orbitals included in RAS3. The results, which are detailed in the Supporting Information, show that the RASSCF calculation with RAS3 limited to one orbital offers the highest computational efficiency while remaining consistent with the [*5*,*3*]_*3* CASSCF/MRCI(5) results.

The RS2 approach[90] of the CASPT2 method has been adopted for adding supplementary correlation effects to the RASSCF {R1[0,0]; R2[5,3]; R3[2,*1*]}_3 results. The occupied orbital space from which excitations are allowed for the second-order perturbation theory treatment has been extended for that purpose to a larger set of orbitals, as compared with the previous RASSCF space. In this case, the total number of correlated orbitals compatible with the MOLPRO code is restricted to a number of 32. This means that 61 electrons are correlated in this way, bringing 1.16 hartree of correlation energy with respect to the RASSCF calculation at the reference 1TC3 geometry. The size of the corresponding configuration space amounts to 7×10^7 contracted CSFs for a CPU time of 3.5 times the [5,3]_3 CASSCF reference calculation. The level of calculation, noted RASSCF/RASPT2(61) in this work, has been used to optimize the reaction path describing the charge transfer process in the stacked dimer $(GG)^+$. The results of the calculations will be presented in Section 4.2.

4. Results and Discussion

4.1. Effects of Translational and Rotational Motions of Guanine $G_{5'}$ on the Charge Transfer in the Radical Cation $(G_{5'}G_{3'})^+$. To estimate how each motion of guanine $G_{5'}$ relative to guanine $G_{3'}$ can affect the charge migration, we calculated the energies and the percentages of the positive charge on the guanines $G_{5'}$ and $G_{3'}$ for a series of configurations where only one of the six intermolecular parameters was changed. These calculations have been performed at the CASSCF/MRCI(5)/6-31G(d(0.2)) level. The results are presented below.

4.1.a. Translational Motions. Figure 3a shows the relative energies of the ground state and of the first excited state computed for the stacked $(G_{5'}G_{3'})^+$ system as a function of the parameters *d*, *q*, and *l*. The energy scale used in this Figure is relative to the ground electronic state of the reference geometry. Although the ground, first, and second excited states of the complex have been calculated in this work, only the ground state and the first excited state are depicted because only those two states describe the charge transfer process between the bases $G_{5'}$ and $G_{3'}$. (See Section 3.) Figure 3b presents the percentages of the positive charge on the guanine $G_{5'}$ (solid line) and on the guanine $G_{3'}$ (dotted line) calculated for the ground state as a function of the parameters *d*, *q*, and *l*. We used the following ranges of the parameters: $d \pm 0.5$ Å, $q \pm 4$ Å, and $l \pm 1.5$ Å. (See the inset of the Figure for the definition of the signs of these parameters.) The large range $q \pm 4$ Å is justified by the

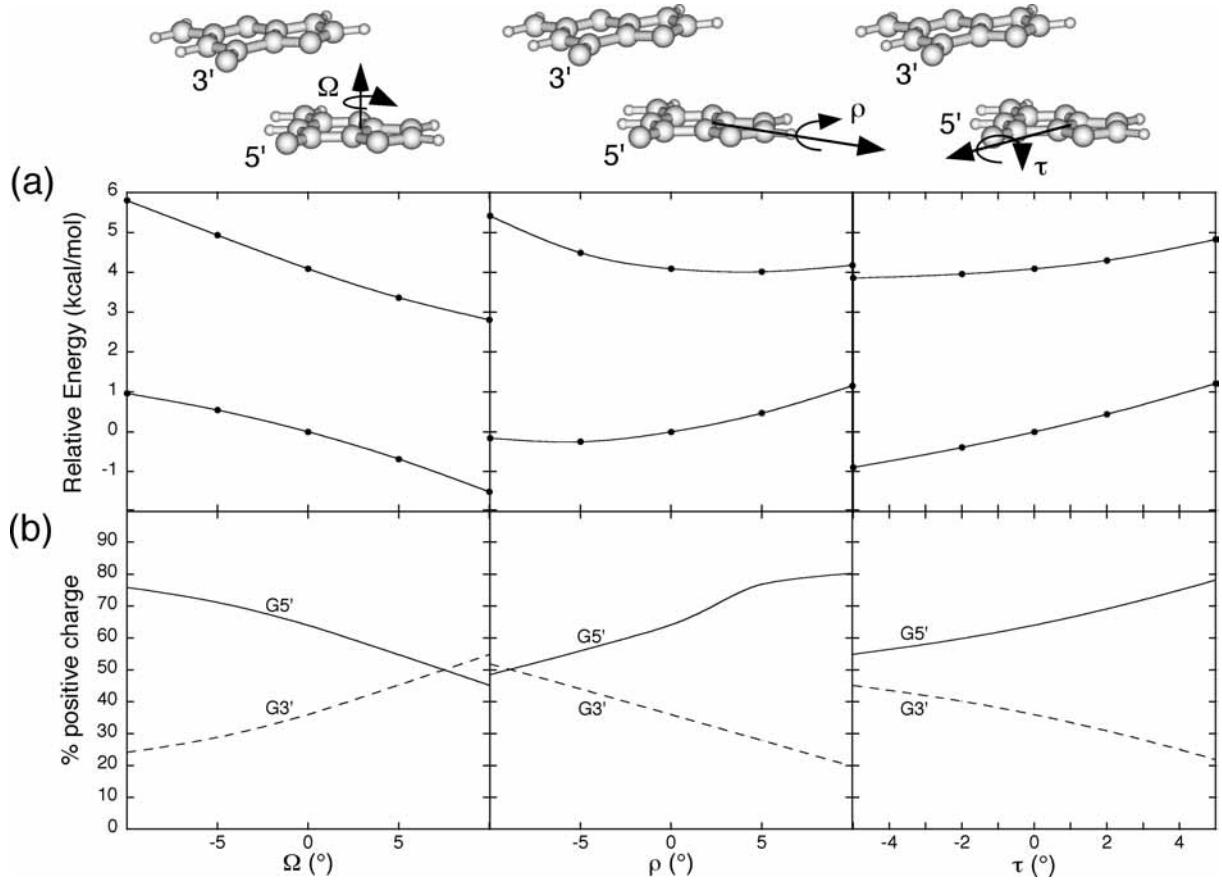

Figure 4. (a) Energies of the ground state and of the first excited state, computed at the CASSCF/MRCI(5)/6-31G(d(0.2)) level for the stacked $(G_{5'}G_{3'})^+$ system as a function of the parameters τ, ρ, and Ω. (b) Percentages of the positive charge on the guanine $G_{5'}$ (solid line) and on the guanine $G_{3'}$ (dotted line) calculated for the ground state as a function of the parameters τ, ρ, and Ω.

extreme value of slide (2.9 Å) in the reference configuration where the bases are essentially unstacked.

A very flat minimum characterizes the ground-state energy curve computed as a function of parameter *d*. We observe that the optimal *d* value is equal to 0.0 Å, that is, the reference configuration, which corresponds to a distance of 3.3 Å between the center of mass of guanine $G_{5'}$ and the molecular plane of guanine $G_{3'}$. For this configuration, 64% of the positive charge is located on $G_{5'}$ and 36% is located on $G_{3'}$. The variation of the parameter *d* does not lead to a significant charge transfer from one guanine to another.

The ground-state energy curve as a function of *q* presents two pronounced minima at values of $q = 0$ and -3 Å, separated by a potential energy barrier. At $q = -3$ Å, the percentages of the positive charge on the guanines $G_{5'}$ and $G_{3'}$ reach 25 and 75%, respectively. The value $q = -3$ Å corresponds to a configuration in which the stacked guanines are essentially superposed. At the top of the potential energy barrier, at $q = -1$ Å, the positive charge is distributed equally between the two nucleobases. This suggests that this point corresponds to the avoiding crossing between the ground and first excited states. The changes of the parameter *q* thus have a significant effect on the distribution of the positive charge in the radical cation $(G_{5'}G_{3'})^+$ and are found to play a significant role in the charge transfer mechanism.

In the case of parameter *l*, although a charge migration between the two guanines is observed, the ground-state energy profile is flat and contains no minima. This result suggests that our CASSCF/MRCI(5) calculations performed with the minimal active orbital space [*5,3*]_*3* do not fully recover the subtle electron correlation associated with motion of $G_{5'}$ along $l^{5'}$. This will be confirmed later in Section 4.2 on the basis of the calculations performed at a higher level of theory.

4.1.b. Rotational Motions. Figure 4a shows the relative energies of the ground state and of the first excited state, computed for the stacked $(G_{5'}G_{3'})^+$ system as a function of the parameters τ, ρ, and Ω. Figure 4b presents the percentages of the positive charge on the guanine $G_{5'}$ (solid line) and on the guanine $G_{3'}$ (dotted line) calculated for the ground state as a function of the parameters τ, ρ, and Ω. The following ranges of the parameters, $\tau \pm 5°$, $\rho \pm 10°$, and $\Omega \pm 10°$, were used. (See the inset of the Figure for the definition of the signs of these parameters.)

The results show that none of the three rotational motions induce a charge transfer. The positive charge remains mainly localized on guanine $G_{5'}$. In each case, the percentage of the positive charge calculated for the ground state on guanine $G_{5'}$ varies between ~50 and 80%. No point on the PES of Figure 4a corresponds to the position of the charge on guanine $G_{3'}$, that is, more than 95% positive charge on this base.

4.2. Topology of the Potential Energy Surface of the Radical Cation $(G_{5'}G_{3'})^+$. The results of preliminary calculations presented in Section 4.1 suggest that both of translation motions of guanine $G_{5'}$ along the axes $l^{5'}$ and $q^{5'}$ can cause the migration of the positive charge from one guanine to the other in the ionized radical $(G_{5'}G_{3'})^+$. However, changes in the vertical separation of the two nucleobases or rotational motions of guanine $G_{5'}$ have essentially no effect on the charge transfer process. To estimate the coupling between the translational modes of guanine $G_{5'}$ along the axes $l^{5'}$ and $q^{5'}$, we calculated

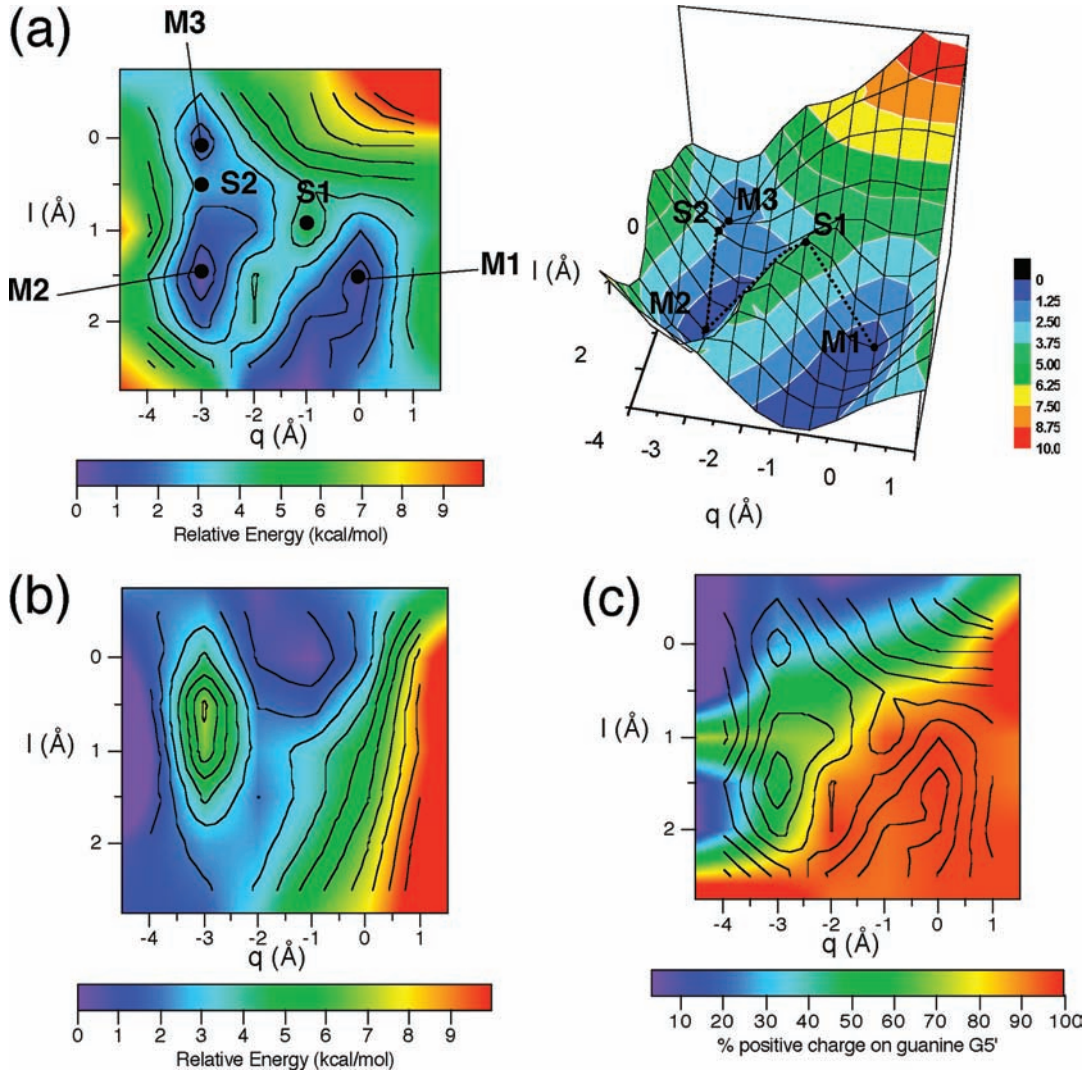

Figure 5. Energy maps for the (a) ground and (b) first excited states calculated at the RASSCF/RASPT2(61)/6-31G(d(0.2)) level for the radical cation $(G_{5'}G_{3'})^+$ as a function of the parameters q and l. The vertical separation between the two stacked guanines is kept fixed equal to 3.3 Å. Five stationary points have been localized (M for minimum, S for saddle point) (c) Percentage of the positive charge on the guanine $G_{5'}$ calculated for the ground state. In each part of the Figure, the point (0,0) corresponds to the reference crystal structure 1TC3.

the energy and the distribution of the charge of the radical cation $(G_{5'}G_{3'})^+$ for a series of configurations with the center of mass of guanine $G_{5'}$ situated at the grid points (l, q) where $-4 \leq q \leq 1$ Å and $-0.5 \leq l \leq 3$ Å. These values are in agreement with deviations predicted by Hunter et al.[97] of slide and shift of ± 4 and ± 2 Å, respectively, and are in agreement with average deviations found by molecular dynamics simulations by Voityuk et al.[57] The following increments have been used: $q \pm 1$ Å and $l \pm 0.5$ Å. The parameters d, τ, ρ, and Ω have been fixed at their reference values. The calculations were performed at the RASSCF/RASPT2(61) level of theory using the 6-31G(d(0.2)) basis set. The resulting relative energies for the ground and first excited states of the radical cation $(G_{5'}G_{3'})^+$ are presented in Figures 5a (2D and 3D representations) and 5b, respectively, as a function of the parameters q and l. Figure 5c shows the percentage of the positive charge on the guanine $G_{5'}$ calculated for the ground state. In each Figure, the point (0,0) corresponds to the reference crystal structure 1TC3. Energy isocontours are plotted over Figure 5a,b. In Figure 5c, the charge distribution is presented in color, whereas the energy isocontours of Figure 5a are redrawn over it.

The topology of the ground-state PES (Figure 5a) shows five stationary points: three minima, denoted M1, M2, and M3, at the coordinates (1.5, 0), (1.5, −3), and (0, −3), respectively, and two saddle points, S1 and S2, at (1, −1) and (0.5, −3), respectively. We see that the minimum M1 is flat and covers a wide range. Three distinct zones are observed in Figure 5c: a first zone surrounding M1 in which the positive charge is essentially on guanine $G_{5'}$, a second zone around M2, that shows a uniform distribution of the charge on both bases, and a third zone close to M3 where the positive charge is on guanine $G_{3'}$. The saddle points S1 and S2 are at the border between the first and the second zones and between the second and the third zones, respectively. The minimum M1 in which 98% of the positive charge is on guanine $G_{5'}$ is more stable by 0.98 kcal/mol than the minimum M3, where 72% of the positive charge is on guanine $G_{3'}$. The height of the potential energy barrier separating M1 and M2 reaches 4.48 kcal/mol. In Figure 5a, it is surprising to see that the stationary points M1 and M2 are on an axis parallel to $q^{5'}$ at $l = 1.5$ Å, whereas M2 and M3 are on an axis parallel to $l^{5'}$ at $q = -3$ Å. The geometrical structures of the complex GG corresponding to the minima M1 and M3 are depicted in Figure 2S of the Supporting Information. Starting from the point M2, a motion of guanine $G_{5'}$ to positive q values leads to a charge transfer to the guanine $G_{5'}$, whereas a movement of $G_{5'}$ in the direction of negative l values results in

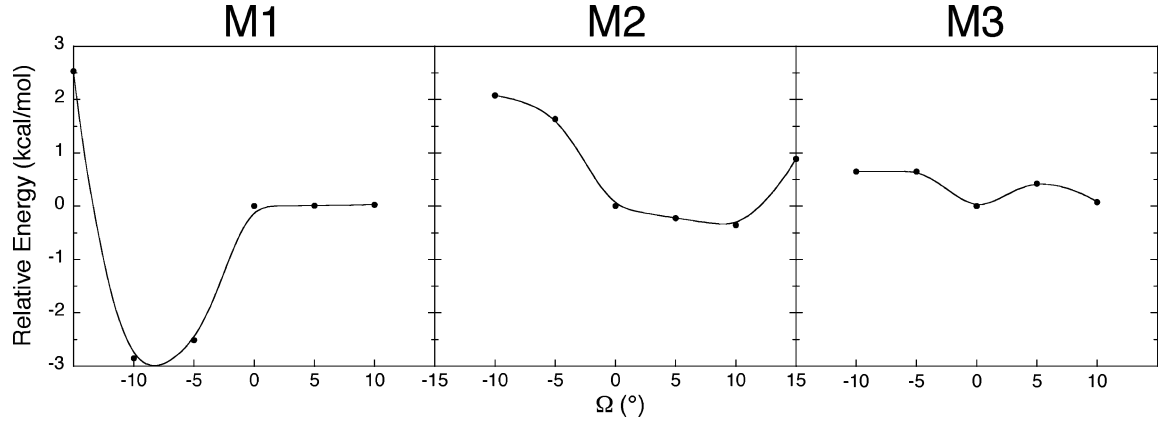

Figure 6. Relative energies of the ground state computed at the RASSCF/RASPT2(61)/6-31G(d(0.2)) level for M1, M2, and M3 as a function of the parameter Ω. The sign of the parameter Ω is indicated in Figure 4.

a charge migration to the guanine $G_{3'}$. According to the model of Prat et al.,[39] this result can be interpreted by the electrostatic potential of the isolated guanine base that shows significant concentration of negative charge on O and N atoms designated by O_{10} and N_7 and O_{26} and N_{23} for $G_{5'}$ and $G_{3'}$, respectively. For our system, M1 corresponds to a configuration in which N_{23} of $G_{3'}$ is located just above the six-membered ring of the $G_{5'}$ stabilizing the cation located in guanine $G_{5'}$. M3 corresponds to N_7 and O_{10} of $G_{5'}$ below the aromatic ring of $G_{3'}$ stabilizing the positive charge on guanine $G_{3'}$.

4.3. Optimization of the Stationary Points. As already pointed out by previous investigations,[67] the variations of twist angle and distance between the guanines have a small effect on the energies of the system. However, these parameters were found to strongly affect charge transfer integrals.[66,67,70] It is for this reason that we decided, for geometrical configurations corresponding to all stationary points M1, M2, M3, S1, and S2, to optimize the parameters d and Ω, characterizing the translation and the rotation of guanine $G_{5'}$ along and around the axes $d^{5'}$, respectively. These were independently optimized at the RASSCF/RASPT2(61)/6-31G(d(0.2)) level.

4.3a. Minima M1, M2, and M3. For each Ω value, the results show that the energy of the complex in M1, M2, and M3 is strongly destabilized by motion along the $d^{5'}$ direction, indicating that the reference structure possesses the most stable d value. Figure 6 presents the relative energies of the ground state computed for M1, M2, and M3 as a function of the parameter Ω with the vertical separation between the stacked guanines kept fixed equal to the reference value, 3.3 Å. The value Ω = 0 corresponds to the orientation of the guanine $G_{5'}$ in the reference structure 1TC3, and the sign of the parameter Ω is indicated in Figure 4. The energy scale used in this Figure is relative to the ground electronic state of the reference geometry.

The curve corresponding to the configuration M1 shows a minimum at an optimal Ω value close to −10°. At this point, the ground-state energy is stabilized by 2.85 kcal/mol. This can be interpreted to be a consequence of the oxygens of the two guanines moving further away from each other. Further rotation of guanine $G_{5'}$ to −15° breaks the $\pi-\pi$ interaction between the two guanines, dramatically increasing the relative energy.

For the structure M2, the rotation of guanine $G_{5'}$ to positive Ω values slightly stabilizes the complex (<0.5 kcal/mol) with an optimal value of Ω equal to +10°. For Ω values greater than +10°, the energy increases as a result of the fact that these geometries effectively prohibit the $\pi-\pi$ interaction between the two bases. The negative rotation of guanine $G_{5'}$ makes the oxygens of the two guanines closer to each other, destabilizing the stack by up to 2.43 kcal/mol relative to the minimal energy.

For M3, although the distance separating the two oxygens varies, the change in energy as a function of parameter Ω does not exceed 0.65 kcal/mol. This can be explained by the fact that the configuration corresponding to the minimum M3 presents two guanines essentially aligned and that rotation of the guanine $G_{5'}$ does not change the overlap between the π clouds of the two aromatic molecules.

The Mulliken populations calculated for each point of the curves M1 and M3 of Figure 6 reveal negligible changes of the distribution of the positive charge between the two guanines. The percentage of the positive charge on guanine $G_{5'}$ varies between 95 and 98% and between 28 and 38% for M1 and M3, respectively. A detailed analysis of the charge density of individual monomers of the complex GG shows only small fluctuations for each atomic charge. The data in M2 present larger charge fluctuations. For Ω ranging from 0 to +10°, 49 to 52% of the positive charge is on guanine $G_{5'}$. For other Ω values, up to 32% more are present on the base. It is essentially the atomic charges of the atoms located on the five-membered rings of the guanines that vary.

4.3b. Saddle Points S1 and S2. The ground-state relative energies, calculated for the structures S1 and S2 as a function of the parameters d and Ω, are presented in Figure 7. The two PESs clearly show a topology characteristic of a saddle point. The energy of the complex increases for any change in d and decreases for any change in Ω. The saddle points are observed at Ω equal to 0 and −5° for structures S1 and S2, respectively, and $d = 0$ Å. At these points, the percentage of positive charge on guanine $G_{5'}$ is 96 and 47% for S1 and S2, respectively.

4.4. Energy Landscape. The main features of the energy landscape characterizing the reaction path that describes the charge transfer in the stacked complex $(G_{5'}G_{3'})^+$ are summarized in Figure 8. The relative energies of the ground and first excited states (Figure 8a) are computed at the RASSCF/RASPT2(61)/6-31G(d(0.2)) level for the five stationary points optimized in the previous sections. Figure 8b displays the percentages of the positive charge on the guanine $G_{5'}$ (solid line) and $G_{3'}$ (dotted line) calculated for the ground state. The optimized geometrical structures corresponding to the five stationary points are depicted in Figure 9. The corresponding Cartesian coordinates are provided in the Supporting Information as Tables 1S−5S.

We observe that the minimum M1, corresponding to the charge configuration $G_{5'}{}^+G_{3'}$, is more stable by 3.84 kcal/mol than the minimum M3 corresponding to the charge configuration $G_{5'}G_{3'}{}^+$. The minimum M2, in which the charge is equally distributed between the two guanines, is destabilized by 2.13 kcal/mol relative to M1. The height of the potential energy barrier between M1 and M2 reaches 7.33 kcal/mol. To calculate

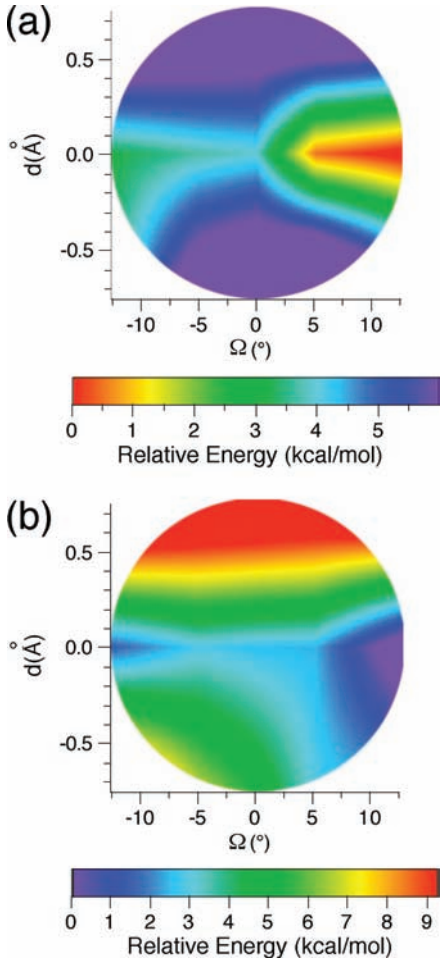

Figure 7. Ground-state relative energy calculated, at the RASSCF/RASPT2(61)/6-31G(d(0.2)) level, for the structures (a) S1 and (b) S2 as a function of the parameters d and Ω.

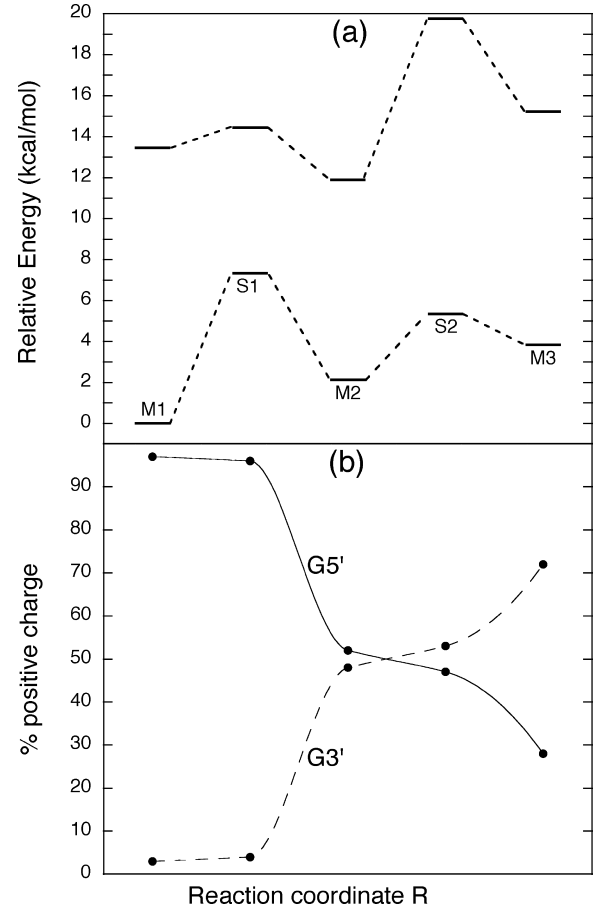

Figure 8. (a) Relative energies of the ground and first excited states computed at the RASSCF/RASPT2(61)/6-31G(d(0.2)) level for the five stationary points optimized (M for minimum, S for saddle point). (b) Percentages of the positive charge on the guanine $G_{5'}$ (solid line) and $G_{3'}$ (dotted line) calculated for the ground state.

the electronic coupling for charge transfer between the stacked guanines, we applied the two-state model of electron transfer at the RASPT2 level. In this procedure, the electronic coupling can be estimated to be half of the minimum splitting between the two adiabatic states, that is, the ground and first excited states. We estimated the half of the minimum splitting at the top of the energy barrier to be 3.6 kcal/mol, providing a valuable estimate of electronic coupling for hole transfer at the optimized geometry close to the avoiding crossing.

The energy profile for electron transfer presented in Figure 8 has been obtained within the approximation of frozen monomer geometries. Going beyond this approximation using large scale RASPT2 calculations is unfortunately out of reach of present computer capabilities. An estimation of the internal reorganization energy has nevertheless been achieved for the three minima: M1, M2, and M3. For each of these structures, we have optimized all intramolecular parameters at the HF/6-31G(d,p) level of theory keeping the intermolecular parameters characterizing these structures fixed. The RASPT2(61)/6-31G(d(0.2)) energies were then recalculated at the optimized geometries. The absolute reorganization energies are found to be less than 4 kcal/mol, and the root-mean-square deviations between initial and optimized structures are small (between 0.03 and 0.07 Å). The results show that optimization of the intramolecular geometrical parameters does not change the stability order of the minima previously found and that the charge transfer still occurs from M1 to M3 (percentages of positive charge on $G_{5'}$ of 97, 43, and 7% for M1, M2, and M3, respectively). However, the relative stability between the three minima has changed. M2 and M3 are destabilized by 3.63 and 6.18 kcal/mol, respectively, relative to M1. This should be compared with 2.13 and 3.84 kcal/mol obtained before internal optimization. These differences should be considered to be indicative only because the optimizations have been performed at the HF level. We would like to stress that geometry relaxation certainly brings small energy shifts along the electron transfer energy path. However, this does not change the global topology of our calculated PES.

4.5. Interaction Energies. To elucidate the relative stability of the stationary points M1 and M3 on the PES of the radical cation $(GG)^+$, the interaction energies were calculated at the MP2 level with the 6-31G(d(0.2)) basis set. The standard counterpoise method was applied to correct the interaction energies for the basis set superposition error. The monoconfigurational theory MP2 could be used only at the geometries M1 and M3, for which the ground-state wave function can be described by one dominant electronic configuration because of the pure distributions of the positive charge obtained for these structures.

The interaction energies of the neutral complexes are −3.50 and −3.88 kcal/mol for the structures M1 and M3, respectively. The structure M3 is found to be the most stable, although the energy difference between the two minima is negligible (<0.4 kcal/mol) because of the delocalization of the π electrons of the aromatic rings of the guanine base. The MP2 calculations performed for the cation species show that M1 is more stable

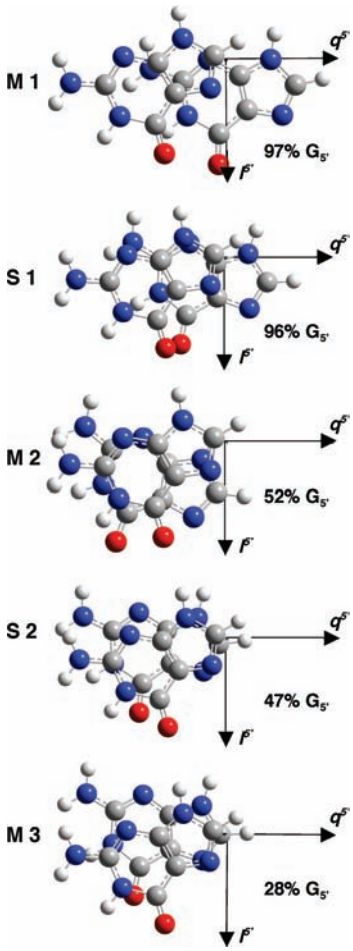

Figure 9. Optimized geometrical structures corresponding to the five stationary points M and S of Figure 8. Atoms O, N, C, and H are colored in red, blue, gray, and white, respectively.

following the ionization. The interaction energies computed for M1 and M3 are −13.79 and −11.77 kcal/mol, respectively. The contributions of the positive charge to the complexes stability, obtained from differences between the energies for neutral and cation species, are significant. They reach 10.29 and 7.89 kcal/mol for the structures M1 and M3, respectively.

5. Conclusions

The charge transfer process in an ionized stacking of two consecutive guanines $(G_{5'}G_{3'})^+$ has been studied by means of multiconfigurational calculations. The ground and two first excited states of the radical cation have been characterized, and the topology of the corresponding PES has been studied as a function of the intermolecular parameters of the DNA base cluster. The level of calculation to be used for a correct description of the electronic states in this system has been carefully investigated on the basis of systematic test calculations. The state-averaged CASSCF/MRCI and state-averaged RASSCF/RASPT2 approaches have been used, providing an accurate representation of the modifications appearing in the wave functions along a reaction coordinate and describing the configurational changes accompanying the charge transfer from one guanine to the other. The 6-31G(d(0.2)) basis set has also been utilized. It presents the advantage of accurately describing both the $\pi-\pi$ interaction between the two guanines and the electronic changes accompanying ionization.

The results demonstrate that the charge transfer process in the ionized stack $(G_{5'}G_{3'})^+$ is mediated by the avoiding crossing between the ground and first excited states of the complex. Two geometrical conformational changes have been emphasized governing the charge migration corresponding to the translation motions of guanine $G_{5'}$ in the molecular plane defined by its aromatic ring. Geometry optimizations have been performed to find the stationary points along the reaction path describing the passage of the positive charge from the guanine $G_{5'}$ to guanine $G_{3'}$. The minimum corresponding to the charge configuration $G_{5'}{}^+G_{3'}$ is more stable than the minimum of the charge configuration $G_{5'}G_{3'}{}^+$. The existence of an intermediate minimum has been established, characterizing a structure where the positive charge is equally distributed between the two guanines. The calculated energy profile allowed us to determine the height of the potential energy barrier (7.33 kcal/mol) and to evaluate the electronic coupling at a geometry close to the avoiding crossing (3.6 kcal/mol). Test calculations showed that the topology of the ground-state PES of the complex GG^+ is conserved upon optimization of the intramolecular geometrical parameters of the stationary points.

The results presented in this article provide a detailed characterization of very specific conformations of the DNA stack required for the charge transfer. They demonstrate how sensitive the charge migration in DNA is to the stacking geometry. In fact this high sensitivity is very important because it has led to the proposal that DNA charge transfer may play a role in detecting DNA damage within the cell.[20] Only two bases were considered in our ab initio calculations of base complexes, but it would be worthwhile to extend our system to larger clusters. Indeed, consideration of longer poly-G sequences is expected to change the relative stability of structures implied in the charge transfer process between two guanines. Also, the survey of such motifs inside the DNA context is necessary to show that the optimized structures found in this work are compatible with the structural constraints provided by the native DNA environment. Both of these studies are in progress and will be part of future papers.

Acknowledgment. The Communauté Française de Belgique (ARC contract) and the FRS-FNRS (Fonds National de la Recherche Scientifique de Belgique, IISN project) are acknowledged for financial support. E.C. is a FNRS researcher. Dr. René Wintjens and Dr. Marianne Rooman are acknowledged for helpful discussions.

Supporting Information Available: Detailed information on the RASSCF methodological tests, geometrical structures corresponding to the minima M1 and M3 of Figure 5, and Cartesian coordinates of the five optimized structures presented in Figure 9. This material is available free of charge via the Internet at http://pubs.acs.org.

References and Notes

(1) *Long-Range Charge Transfer in DNA I*; Schuster, G. B., Ed.; Topics in Current Chemistry 236; Springer: New York, 2004.
(2) *Long-Range Charge Transfer in DNA II*; Schuster, G. B., Ed.; Topics in Current Chemistry 237; Springer: New York, 2004.
(3) *Charge Transfer in DNA: From Mechanism to Application*; Wagenknecht, W. A., Ed.; Wiley-VCH: Weinheim, Germany, 2005.
(4) Sabin, J. R. Theoretical Studies of the Interaction of Radiation with Biomolecules. In *Advances in Quantum Chemistry*; Sabin, J. R., Ed.; Academic Press: New York, 2007; Vol. 52.
(5) Endres, R. G.; Cox, D. L.; Singh, R. R. P. *Rev. Mod. Phys.* **2004**, *76*, 195.
(6) Porath, D.; Cuniberti, G.; Di Felice, R. *Top. Curr. Chem.* **2004**, *237*, 183.
(7) Guo, X.; Gorodetsky, A. A.; Hone, J.; Barton, J. K.; Nuckolls, C. *Nat. Nanotechnol.* **2008**, *3*, 163.
(8) Ye, Y. J.; Jiang, Y. *Int. J. Quantum Chem.* **2000**, *78*, 112.

(9) Treadway, C. R.; Hill, M. G.; Barton, J. K. *Chem. Phys.* **2002**, *281*, 409.
(10) Meggers, E.; Michel-Beyerle, M. E.; Giese, B. *J. Am. Chem. Soc.* **1998**, *120*, 12950.
(11) Jortner, J.; Bixon, M.; Langenbacher, T.; Michel-Beyerle, M. E. *Proc. Natl. Acad. Sci. U.S.A.* **1998**, *95*, 12759.
(12) Giese, B. *Acc. Chem. Res.* **2000**, *33*, 631.
(13) Berlin, Y. A.; Burin, A. L.; Ratner, M. A. *J. Am. Chem. Soc.* **2001**, *123*, 260.
(14) Giese, B. *Annu. Rev. Biochem.* **2002**, *71*, 51.
(15) Giese, B. *Top. Curr. Chem.* **2004**, *236*, 27.
(16) Schuster, G. B. *Acc. Chem. Res.* **2000**, *33*, 253.
(17) Lewis, F. D.; Letsinger, R. L.; Wasielewski, M. R. *Acc. Chem. Res.* **2001**, *34*, 159.
(18) Giese, B. *Curr. Opin. Chem. Biol.* **2002**, *6*, 612.
(19) O'Neill, M. A.; Barton, J. K. *Top. Curr. Chem.* **2004**, *236*, 67.
(20) Merino, E. J.; Boal, A. K.; Barton, J. K. *Curr. Opin. Chem. Biol.* **2008**, *12*, 229.
(21) Elias, B.; Genereux, J. C.; Barton, J. K. *Angew. Chem., Int. Ed.* **2008**, *47*, 9067.
(22) Elias, B.; Shao, F.; Barton, J. K. *J. Am. Chem. Soc.* **2008**, *130*, 1152.
(23) Giese, B.; Spichty, M. *ChemPhysChem* **2000**, *1*, 195.
(24) Grozema, F. C.; Berlin, Y. A.; Siebbeles, L. D. A. *J. Am. Chem. Soc.* **2000**, *122*, 10903.
(25) Bixon, M.; Jortner, J. *J. Phys. Chem. A* **2001**, *105*, 10322.
(26) Berlin, Y. A.; Burin, A. L.; Ratner, M. A. *Chem. Phys.* **2002**, *275*, 61.
(27) Berlin, Y. A.; Kurnikov, I. V.; Beratan, D. N.; Ratner, M. A.; Burin, A. L. *Top. Curr. Chem.* **2004**, *237*, 1.
(28) Rösch, N.; Voityuk, A. A. *Top. Curr. Chem.* **2004**, *237*, 37.
(29) Voityuk, A. A. *J. Chem. Phys.* **2005**, *123*, 034903.
(30) Voityuk, A. A. *Chem. Phys. Lett.* **2008**, *451*, 153.
(31) Voityuk, A. A. *J. Chem. Phys.* **2008**, *128*, 115101.
(32) Colson, A. O.; Besler, B.; Close, D. M.; Sevilla, M. D. *J. Phys. Chem.* **1992**, *96*, 661.
(33) Colson, A. O.; Besler, B.; Sevilla, M. D. *J. Phys. Chem.* **1993**, *97*, 13852.
(34) Hutter, M.; Clark, T. *J. Am. Chem. Soc.* **1996**, *118*, 7574.
(35) Bertran, J.; Oliva, A.; Rodriguez-Santiago, L.; Sodupe, M. *J. Am. Chem. Soc.* **1998**, *120*, 8159.
(36) Li, X.; Cai, Z.; Sevilla, M. D. *J. Phys. Chem. B* **2001**, *105*, 10115.
(37) Li, X.; Cai, Z.; Sevilla, M. D. *J. Phys. Chem. A* **2002**, *106*, 9345.
(38) Sugiyama, H.; Saito, I. *J. Am. Chem. Soc.* **1996**, *118*, 7063.
(39) Prat, F.; Houk, K. N.; Foote, C. S. *J. Am. Chem. Soc.* **1998**, *120*, 845.
(40) Saito, I.; Nakamura, T.; Nakatani, K.; Yoshioka, Y.; Yamaguchi, K.; Sugiyama, H. *J. Am. Chem. Soc.* **1998**, *120*, 12686.
(41) Yoshioka, Y.; Kitagawa, Y.; Takano, Y.; Yamaguchi, K.; Nakamura, T.; Saito, I. *J. Am. Chem. Soc.* **1999**, *121*, 8712.
(42) Voityuk, A. A.; Jortner, J.; Bixon, M.; Rösch, N. *Chem. Phys. Lett.* **2000**, *324*, 430.
(43) Schumm, S.; Prévost, M.; Garcia-Fresnadillo, D.; Lentzen, O.; Moucheron, C.; Kirsch-De Mesmaeker, A. *J. Phys. Chem. B* **2002**, *106*, 2763.
(44) Cauët, E.; Dehareng, D.; Liévin, J. *J. Phys. Chem. A* **2006**, *110*, 9200.
(45) Cauët, E.; Liévin, J. *Adv. Quantum Chem.* **2007**, *52*, 121.
(46) Conwell, E. M.; Basko, D. M. *J. Am. Chem. Soc.* **2001**, *123*, 11441.
(47) Olofsson, J.; Larsson, S. *J. Phys. Chem. B* **2001**, *105*, 10398.
(48) Kurnikov, I. V.; Tong, G. S. M.; Madrid, M.; Beratan, D. N. *J. Phys. Chem. B* **2002**, *106*, 7.
(49) Senthilkumar, K.; Grozema, F. C.; Guerra, C. F.; Bickelhaupt, F. M.; Siebbeles, L. D. A. *J. Am. Chem. Soc.* **2003**, *125*, 13658.
(50) Voityuk, A. A. *J. Phys. Chem. B* **2005**, *109*, 10793.
(51) Voityuk, A. A. *J. Phys. Chem. B* **2005**, *109*, 17917.
(52) Newton, M. D. *Chem. Rev.* **1991**, *91*, 767.
(53) Voityuk, A. A. *J. Chem. Phys.* **2006**, *124*, 064505.
(54) Voityuk, A. A. *Chem. Phys. Lett.* **2006**, *422*, 15.
(55) Voityuk, A. A. *Chem. Phys. Lett.* **2007**, *439*, 162.
(56) Voityuk, A. A.; Rösch, N.; Bixon, M.; Jortner, J. *J. Phys. Chem. B* **2000**, *104*, 9740.
(57) Voityuk, A. A.; Siriwong, K.; Rösch, N. *Phys. Chem. Chem. Phys.* **2001**, *3*, 5421.
(58) Voityuk, A. A.; Jortner, J.; Bixon, M.; Rösch, N. *J. Chem. Phys.* **2001**, *114*, 5614.
(59) Troisi, A.; Orlandi, G. *Chem. Phys. Lett.* **2001**, *344*, 509.
(60) Troisi, A.; Orlandi, G. *J. Phys. Chem. B* **2002**, *106*, 2093.
(61) Blancafort, L.; Voityuk, A. A. *J. Phys. Chem. A* **2006**, *110*, 6426.
(62) Blancafort, L.; Voityuk, A. A. *J. Phys. Chem. A* **2007**, *111*, 4714.
(63) Félix, M.; Voityuk, A. A. *J. Phys. Chem. A* **2008**, *112*, 9043.
(64) Voityuk, A. A. *Chem. Phys. Lett.* **2006**, *427*, 177.
(65) Sadowska-Aleksiejew, A.; Rak, J.; Voityuk, A. A. *Chem. Phys. Lett.* **2006**, *429*, 546.
(66) Grozema, F. C.; Siebbeles, L. D. A.; Berlin, Y. A.; Ratner, M. A. *ChemPhysChem* **2002**, *3*, 536.
(67) Senthilkumar, K.; Grozema, F. C.; Guerra, C. F.; Bickelhaupt, F. M.; Lewis, F. D.; Berlin, Y. A.; Ratner, M. A.; Siebbeles, L. D. A. *J. Am. Chem. Soc.* **2005**, *127*, 14894.
(68) Kubar, T.; Elstner, M. *J. Phys. Chem. B* **2008**, *112*, 8788.
(69) Voityuk, A. A. *J. Chem. Phys.* **2008**, *128*, 045104.
(70) Kubar, T.; Woiczikowski, P. B.; Cuniberti, G.; Elstner, M. *J. Phys. Chem. B* **2008**, *112*, 7937.
(71) Grozema, F. C.; Tonzani, S.; Berlin, Y. A.; Schatz, G. C.; Siebbeles, L. D. A.; Ratner, M. A. *J. Am. Chem. Soc.* **2008**, *130*, 5157.
(72) Rooman, M.; Liévin, J.; Buisine, E.; Wintjens, R. *J. Mol. Biol.* **2002**, *319*, 67.
(73) Wintjens, R.; Biot, C.; Rooman, M.; Liévin, J. *J. Phys. Chem. A* **2003**, *107*, 6249.
(74) Ditchfield, R.; Hehre, W.; Pople, J. A. *J. Chem. Phys.* **1971**, *54*, 724.
(75) Hariharan, P. C.; Pople, J. A. *Theor. Chim. Acta* **1973**, *28*, 213.
(76) Hobza, P.; Sponer, J. *Chem. Rev.* **1999**, *99*, 3247.
(77) Wintjens, R.; Liévin, J.; Rooman, M.; Buisine, E. *J. Mol. Biol.* **2000**, *302*, 395.
(78) Hobza, P.; Sponer, J. *J. Am. Chem. Soc.* **2002**, *124*, 11802.
(79) Cauët, E.; Rooman, M.; Wintjens, R.; Liévin, J.; Biot, C. *J. Chem. Theory Comput.* **2005**, *1*, 472.
(80) Mignon, P.; Loverix, S.; Geerlings, P. *Chem. Phys. Lett.* **2005**, *401*, 40.
(81) Dickerson, R. E. *Nucl. Acids. Res.* **1989**, *17*, 1797.
(82) Ruedenberg, K.; Cheung, L. M.; Elbert, S. T. *Int. J. Quantum Chem.* **1979**, *16*, 1068.
(83) Roos, B. O. *Int. J. Quantum Chem. Symp.* **1980**, *175*, 14.
(84) Roos, B. O.; Taylor, P.; Siegbahn, P. E. M. *Chem. Phys.* **1980**, *48*, 157.
(85) Olsen, J.; Roos, B. O.; Jorgensen, P.; Jensen, H. J. A. *J. Chem. Phys.* **1988**, *89*, 2185.
(86) Knowles, P. J.; Werner, H. J. *Chem. Phys. Lett.* **1988**, *145*, 514.
(87) Werner, H. J.; Knowles, P. J. *J. Chem. Phys.* **1988**, *89*, 5803.
(88) Andersson, K.; Malmqvist, P.-A.; Roos, B. O.; Sadlej, A. J.; Wolinski, K. *J. Phys. Chem.* **1990**, *94*, 5483.
(89) Andersson, K.; Malmqvist, P.-A.; Roos, B. O. *J. Chem. Phys.* **1992**, *96*, 1218.
(90) Werner, H. J. *Mol. Phys.* **1996**, *89*, 645.
(91) Amos, R. D.; Bernhardsson, A.; Berning, A.; Celani, P.; Cooper, D. L.; Deegan, M. J. O.; Dobbyn, A. J.; Eckert, F.; Hampel, C.; Hetzer, G.; Knowles, P. J.; Korona, T.; Lindh, R.; Lloyd, A. W.; McNicholas, S. J.; Manby, F. R.; Meyer, W.; Mura, M. E.; Nicklass, A.; Palmieri, P.; Pitzer, R.; Rauhut,; Schütz, M.; Schumann, U.; Stoll, H.; Stone, A. J.; Tarroni, R.; Thorsteinsson, T.; Werner, H. J. *MOLPRO: A Package of Ab Initio Programs*, version 2002.1; University of Birmingham: Birmingham, U.K., 2001.
(92) Mulliken, R. S. *J. Chem. Phys.* **1962**, *36*, 3428.
(93) Møller, C.; Plesset, M. S. *Phys. Rev.* **1934**, *46*, 618.
(94) Head-Gordon, M.; Pople, J. A.; Frisch, M. J. *Chem. Phys. Lett.* **1988**, *153*, 503.
(95) Boys, S. F.; Bernardi, F. *Mol. Phys.* **1970**, *19*, 553.
(96) Frisch, M. J., Trucks, G. W.; Schlegel, H. B.; Scuseria, G. E.; Robb, M. A.; Cheeseman, J. R.; Montgomery, J. A., Jr.; Vreven, T.; Kudin, K. N.; Burant, J. C.; Millam, J. M.; Iyengar, S. S.; Tomasi, J.; Barone, V.; Mennucci, B.; Cossi, M.; Scalmani, G.; Rega, N.; Petersson, G. A.; Nakatsuji, H.; Hada, M.; Ehara, M.; Toyota, K.; Fukuda, R.; Hasegawa, J.; Ishida, M.; Nakajima, T.; Honda, Y.; Kitao, O.; Nakai, H.; Klene, M.; Li, X.; Knox, J. E.; Hratchian, H. P.; Cross, J. B.; Bakken, V.; Adamo, C.; Jaramillo, J.; Gomperts, R.; Stratmann, R. E.; Yazyev, O.; Austin, A. J.; Cammi, R.; Pomelli, C.; Ochterski, J. W.; Ayala, P. Y.; Morokuma, K.; Voth, G. A.; Salvador, P.; Dannenberg, J. J.; Zakrzewski, V. G.; Dapprich, S.; Daniels, A. D.; Strain, M. C.; Farkas, O.; Malick, D. K.; Rabuck, A. D.; Raghavachari, K.; Foresman, J. B.; Ortiz, J. V.; Cui, Q.; Baboul, A. G.; Clifford, S.; Cioslowski, J.; Stefanov, B. B.; Liu, G.; Liashenko; A.; Piskorz, P.; Komaromi, I.; Martin, R. L.; Fox, D. J.; Keith, T.; Al-Laham, M. A.; Peng, C. Y.; Nanayakkara, A.; Challacombe, M.; Gill, P. M. W.; Johnson, B.; Chen, W.; Wong, M. W.; Gonzalez, C.; Pople, J. A. *Gaussian 03*, revision C.02; Gaussian, Inc.: Wallingford, CT, 2004.
(97) Hunter, C. A.; Lu, X.-J. *J. Mol. Biol.* **1997**, *265*, 603.

JP902426P